

# A Mitogen-Activated Protein Kinase Cascade Regulating Infection-Related Morphogenesis in *Magnaporthe grisea* <sup>W</sup>

Xinhua Zhao,<sup>1</sup> Yangseon Kim,<sup>1</sup> Gyungsoon Park, and Jin-Rong Xu<sup>2</sup>

Department of Botany and Plant Pathology, Purdue University, West Lafayette, Indiana 47907

Many fungal pathogens invade plants by means of specialized infection structures called appressoria. In the rice (*Oryza sativa*) blast fungus *Magnaporthe grisea*, the pathogenicity mitogen-activated protein (MAP) kinase1 (*PMK1*) kinase is essential for appressorium formation and invasive growth. In this study, we functionally characterized the *MST7* and *MST11* genes of *M. grisea* that are homologous with the yeast MAP kinase kinase *STE7* and MAP kinase kinase kinase *STE11*. Similar to the *pmk1* mutant, the *mst7* and *mst11* deletion mutants were nonpathogenic and failed to form appressoria. When a dominant *MST7* allele with S212D and T216E mutations was introduced into the *mst7* or *mst11* mutant, appressorium formation was restored in the resulting transformants. *PMK1* phosphorylation also was detected in the vegetative hyphae and appressoria of transformants expressing the *MST7*<sup>S212D T216E</sup> allele. However, appressoria formed by these transformants failed to penetrate and infect rice leaves, indicating that constitutively active *MST7* only partially rescued the defects of the *mst7* and *mst11* mutants. The intracellular cAMP level was reduced in transformants expressing the *MST7*<sup>S212D T216E</sup> allele. We also generated *MST11* mutant alleles with the sterile alpha motif (SAM) and Ras-association (RA) domains deleted. Phenotype characterizations of the resulting transformants indicate that the SAM domain but not the RA domain is essential for the function of *MST11*. These data indicate that *MST11*, *MST7*, and *PMK1* function as a MAP kinase cascade regulating infection-related morphogenesis in *M. grisea*. Although no direct interaction was detected between *PMK1* and *MST7* or *MST11* in yeast two-hybrid assays, a homolog of yeast *STE50* in *M. grisea* directly interacted with both *MST7* and *MST11* and may function as the adaptor protein for the *MST11*-*MST7*-*PMK1* cascade.

## INTRODUCTION

In eukaryotic cells, the mitogen-activated protein (MAP) kinases are involved in transducing a variety of extracellular signals and regulating growth and differentiation processes (Gustin et al., 1998; Dohlman, 2002). The MAP kinases (MAPK) are usually activated by MAPK kinases (MEK) that are in turn activated by MEK kinases (MEKK). These MEKK-MEK-MAPK cascades are conserved in eukaryotes and have been studied extensively in various organisms. In *Saccharomyces cerevisiae*, five MAPK genes regulate mating, filamentous growth, high osmolarity response, maintenance of cellular integrity, and ascospore formation (Gustin et al., 1998; Dohlman, 2002). The best characterized MAPK pathway in all organisms is the yeast pheromone response pathway, which is initiated by the binding of mating pheromones to a receptor and the release of stimulatory G $\beta$  subunits. The liberated G $\beta$  directly associates with a scaffold protein, Ste5, and a p21-activated kinase (PAK), Ste20, and is essential for activating the MEKK Ste11, which activates the MEK

Ste7. Downstream from Ste7, Fus3 and Kss1 are two partially redundant MAPKs regulating the mating process (Kusari et al., 2004). Several elements of the pheromone response pathway, including kinases Ste20, Ste11, Ste7, and Kss1, also are involved in filamentous growth in *S. cerevisiae* (Cherkasova et al., 2003).

The ascomycete *Magnaporthe grisea* is pathogenic to economically important crops such as rice (*Oryza sativa*), barley (*Hordeum vulgare*), wheat (*Triticum aestivum*), and millet (*Panicum miliaceum*), and it has emerged as a model system for the study of fungus–plant interactions (Valent and Chumley, 1991; Talbot, 2003). On plant leaf or artificial hydrophobic surfaces, germ tubes produced from conidia differentiate into specialized infection structures called appressoria. The fungus generates enormous turgor pressure in appressoria to penetrate the underlying plant surface. After penetration, the peg differentiates into bulbous, lobed infectious hyphae that result in the development of blast lesions. In the past few years, several signal transduction pathways regulating surface recognition, appressorium formation, and invasive growth in *M. grisea* have been identified (Dean, 1997; Talbot, 2003). The cAMP signaling pathway is involved in surface recognition and appressorium turgor generation (Mitchell and Dean, 1995; Xu et al., 1997; Thines et al., 2000). *PMK1* (for *PATHOGENICITY MAP KINASE1*), a homolog of yeast *FUS3/KSS1*, regulates appressorium formation and infectious hyphal growth (Xu and Hamer, 1996). Germ tubes of *pmk1* mutants fail to form appressoria but still recognize hydrophobic surfaces or respond to exogenous cAMP and produce subapical swollen bodies. Another MAPK gene, *MPS1*, is homologous with *S. cerevisiae* *SLT2* and required for

<sup>1</sup> These authors contributed equally to this work.

<sup>2</sup> To whom correspondence should be addressed. E-mail jinrong@purdue.edu; fax 765-496-6918.

The author responsible for distribution of materials integral to the findings presented in this article in accordance with the policy described in the Instructions for Authors (www.plantcell.org) is: Jin-Rong Xu (jinrong@purdue.edu).

<sup>W</sup>Online version contains Web-only data.

Article, publication date, and citation information can be found at www.plantcell.org/cgi/doi/10.1105/tpc.104.029116.

cell wall integrity and appressorial penetration in *M. grisea* (Xu et al., 1998). The *mps1* mutant is significantly reduced in aerial hyphal growth and conidiation. Colonies formed by the *mps1* mutant on oatmeal agar plates undergo autolysis when cultures are older than 4 d (Xu et al., 1998).

In the past few years, MAPK genes homologous with *PMK1* have been characterized in several phytopathogenic fungi. The *PMK1* homologs are essential for appressorium formation in all four appressorium-forming fungal pathogens examined to date: *M. grisea*, *Colletotrichum lagenarium*, *Cochliobolus heterostrophus*, and *Pyrenophora teres* (Lev et al., 1999; Takano et al., 2000; Ruiz-Roldan et al., 2001). In *Colletotrichum gloeosporioides*, *CgMEK1* encodes a MEK that is required for appressorium formation and virulence (Kim et al., 2000). Similar to *pmk1* mutants in *M. grisea*, gene replacement mutants of *PTK1* in *P. teres* and *CMK1* in *C. lagenarium* are nonpathogenic and fail to colonize healthy or wounded host tissues (Takano et al., 2000; Ruiz-Roldan et al., 2001). *PMK1* homologs are also important for fungal pathogenicity in several filamentous ascomycetes, including *Botrytis cinerea*, *Gibberella zeae*, *Fusarium oxysporum* f sp *lycopersici*, and *Claviceps purpurea* (Di Pietro et al., 2001; Mey et al., 2002; Jenczmionka et al., 2003). In the basidiomycete *Ustilago maydis*, two MAPKs, *ubc3* (*kpp2*) and *kpp6*, are similar to other fungal MAPKs involved in mating and pathogenicity (Kahmann and Kamper, 2004). The *ubc3* (*kpp2*) disruption mutants are reduced in virulence and mating but still infect plants and form tumors (Mayorga and Gold, 1999; Muller et al., 1999). The *kpp6* deletion mutants are also reduced in virulence and are defective in the penetration of the plant cuticle (Brachmann et al., 2003). However, the *kpp2 kpp6* double mutants are abolished in mating and fail to induce disease symptoms on maize plants. These studies indicate that the *PMK1* pathway may be well conserved in many phytopathogenic fungi for regulating appressorium formation and other plant infection processes.

In this study, we characterized the *M. grisea* *MST7* and *MST11* genes that were homologs of yeast *Ste7* MEK and *Ste11* MEKK. Similar to the *pmk1* mutant, mutants with *MST7* or *MST11* deleted failed to form appressoria and failed to colonize rice tissues through wounds. Expression of a dominant active *MST7* allele partially rescued the defects of the *mst7* and *mst11* mutants. Phosphorylation of *Pmk1* was detected in transformants expressing the dominant active *MST7* allele. These data indicate that *MST11* and *MST7* function as the MEKK and MEK that activate *PMK1* in *M. grisea*. A homolog of yeast *Ste50* and *U. maydis* *Ubc2* directly interacted with both *Mst7* and *Mst11* and may function as the adaptor protein for the *MST11-MST7-PMK1* cascade.

## RESULTS

### *MST7* MEK and *MST11* MEKK Genes

The *M. grisea* genome has three putative MEKK and three putative MEK genes. Based on their homology with yeast homologs, these *M. grisea* MEKKs and MEKs together with three known MAPKs could be assigned to three MAPK cascades homologous with the yeast *FUS3/KSS1*, *HOG1*, and *SLT2* pathways. *MST7* and *MST11* are homologs of yeast *STE7* and *STE11*, respectively, in *M. grisea*. Similar to *STE11* and its homologs

from other fungi, *MST11* also contains an N-terminal sterile alpha motif (SAM) domain and a C-terminal protein kinase domain (Figure 1A). Downstream from the SAM domain, *MST11* has a Ras-association (RA) domain, which is well conserved in its homologs from *Neurospora crassa* and *Fusarium graminearum*.

To determine their functions in *M. grisea*, we generated mutants with the *MST7* and *MST11* genes deleted. The *MST11*

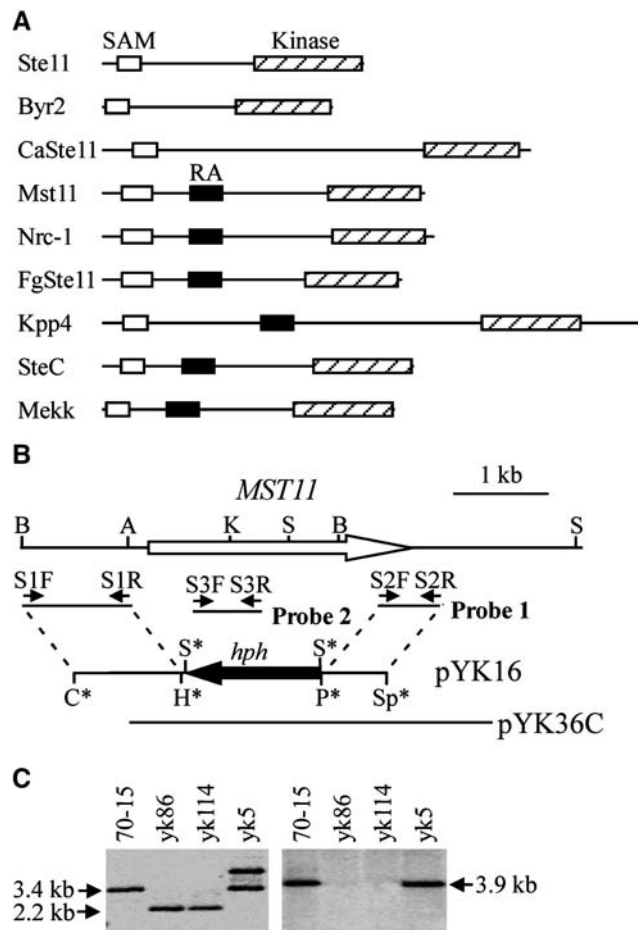


**Figure 1.** *MST11* and *mst11* Gene Replacement Mutants.

**(A)** Schematic organizations of *MST11* from *M. grisea* and its homologs from other fungi: *S. cerevisiae* Ste11, *S. pombe* Byr2, *C. neoformans* CnSte11, *U. maydis* Kpp4, *A. nidulans* SteC, *P. carinii* MeKK, *N. crassa* Nrc-1, and *F. graminearum* FgSte11. The SAM, RA, and catalytic protein kinase domains are represented by open, closed, and hatched boxes, respectively.

**(B)** PCR primers used to generate the *MST11* gene replacement construct pYK16, and mutants marked with small arrows. Restriction enzyme sites were as follows: A, *Apal*; B, *Bam*HI; C, *Clal*; H, *Hind*III; K, *Kpn*I; P, *Pst*I; S, *Sal*I; Sp, *Spe*I. Enzyme sites introduced during the cloning process are labeled with asterisks.

**(C)** DNA gel blot analyses of the wild-type strain (70-15), two *mst11* deletion mutants (yk86 and yk114), and an ectopic transformant (yk5). DNA samples were digested with *Sal*I and probed with probe 1 (left). The *mst11* deletion mutants had a 2.2-kb instead of the 3.4-kb band. For the blot at right, DNA samples were digested with *Bam*HI and hybridized with probe 2.

gene replacement vector pYK16 (Figure 1B) was constructed by replacing the *MST11* open reading frame (ORF) with the *hph* gene and transformed into the wild-type strain 70-15. Two *mst11* deletion mutants, yk86 and yk114, were identified and confirmed by DNA gel blot hybridization (Figure 1C). The *MST7* gene replacement construct (Figure 2A) was generated by ligation PCR (Zhao et al., 2004). The resulting PCR product was directly transformed into 70-15. One *mst7* gene replacement mutant, ZH32, was identified (Figure 2B). The *mst7* and *mst11* deletion mutants were viable and their growth rates on regular oatmeal agar plates were similar to that of the wild-type strain 70-15 (Table 1). However, they produced much less aerial hyphae and conidia on oatmeal agar plates than did 70-15 (data not shown). Vegetative hyphae of the *mst7* and *mst11* mutants released abundant protoplasts after 20 min of digestion with lysing enzymes (see Supplemental Figure 1 online). Under the same conditions, mycelia of 70-15 produced only a few protoplasts. These data indicate that the *mst7* and *mst11* mutants had weakened cell walls and were more sensitive to cell wall-degrading enzymes than was 70-15.

### *MST7* and *MST11* Are Essential for Appressorium Formation and Plant Infection

Similar to the *pmk1* mutant of Guy11, the *mst7* and *mst11* mutants failed to form appressoria on hydrophobic surfaces (Table 1) but developed subapical swollen bodies (Figure 3A),

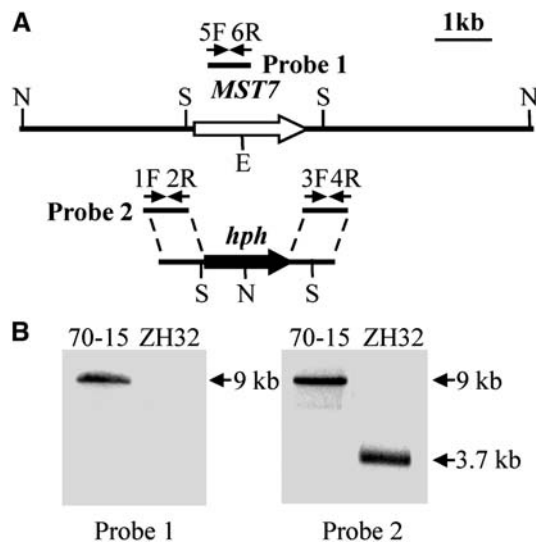


**Figure 2.** *MST7* Gene Replacement Vector and Mutant.

(A) The *MST7* gene replacement construct was constructed by amplifying the upstream and downstream flanking sequences with primers 1F/2R and 3F/4R and ligated with the *hph* cassette. Probe 1 and probe 2 are PCR fragments amplified with primers 5F/6R and 1F/2R. Restriction enzymes were as follows: E, *EcoRI*; N, *NcoI*; S, *SmaI*.

(B) Blots of *NcoI*-digested genomic DNAs of the wild-type strain (70-15) and the *mst7* deletion mutant ZH32 were hybridized with probe 1 (left) or probe 2 (right). The 9-kb band hybridized to probe 1 in 70-15 was absent in ZH32. Probe 2 detected a 9-kb band in 70-15 but a 3.7-kb band in ZH32.

**Table 1.** Growth Rate and Appressorium Formation of *M. grisea* Strains

Strain	Growth Rate (mm/d)		Appressorium Formation (%) <sup>a</sup>	Appressorium Size (μm) <sup>b</sup>
	Oatmeal	+1 M Sorbitol		
70-15	6.0 ± 0.1	3.4 ± 0.1	95.6 ± 1.3	10.3 ± 0.2
yk86	6.2 ± 0.2	1.9 ± 0.1	0	/
ZH32	6.2 ± 0.2	2.2 ± 0.1	0	/
yk86C	6.1 ± 0.1	3.2 ± 0.2	95.1 ± 2.7	10.1 ± 0.4
ZH32C	6.0 ± 0.2	3.2 ± 0.1	93.8 ± 3.3	10.3 ± 0.4
DA5	5.7 ± 0.1	2.4 ± 0.1	88.2 ± 4.8	8.2 ± 0.3
DA3-4	5.8 ± 0.2	3.2 ± 0.1	61.2 ± 3.1	8.0 ± 0.3
DP5	6.0 ± 0.2	N/A <sup>c</sup>	0	/
yk18	5.5 ± 0.1	2.8 ± 0.1	0	/

<sup>a</sup> Percentage of germ tubes formed appressoria by 24 h.

<sup>b</sup> Measured as the average diameter of appressoria formed on plastic cover slips by 24 h. Means and standard errors were calculated from three independent repeats (at least 100 appressoria were measured in each repeat).

<sup>c</sup> Not assayed.

indicating that these mutants had no defect in surface recognition. In the presence of 10 mM cAMP, subapical swollen bodies also were developed by the *mst7* and *mst11* mutants on hydrophilic surfaces (data not shown). Because mutant nn78 was generated in the wild-type strain Guy11, in this study we also generated a *pmk1* deletion mutant of 70-15 (yk18) by transformation with the *PMK1* gene replacement vector pSSE3 (Xu and Hamer, 1996). The phenotype of yk18 was similar to that of nn78 and ZH32 (Figure 3, Table 1).

We assayed the virulence of the *mst7* and *mst11* mutants on rice seedlings. On rice leaves sprayed with conidia of the *mst7* and *mst11* mutants, no lesions were observed at 7 d after inoculation (Figure 3B). The wild-type strain caused numerous lesions under the same conditions (Figure 3B). Rice seedlings also were injected with conidia of the *mst7* and *mst11* mutants. Only restricted necrotic spots at the wound sites were observed on leaves inoculated with the *mst7* and *mst11* mutants at 7 d after inoculation (Figure 3C). In the control experiments, 70-15 caused lesions at and around the wound sites. The *buf1* mutant, which is defective in appressorium turgor generation (Chumley and Valent, 1990), caused only expanding necrosis at the wound sites (Figure 3C). Similar results were obtained in infection assays with seedlings of barley cv Golden Promise (data not shown), indicating that the *mst7* and *mst11* mutants exhibited the same complex spectrum of pathogenicity defects as the *pmk1* mutant. Therefore, *MST11* and *MST7* are likely the MEKK and MEK that activate *PMK1* for appressorium formation and plant infection.

### Cosegregation and Complementation Assays

To confirm that phenotypes observed in the *mst7* and *mst11* mutants were caused by deletion of the *MST7* and *MST11* genes, we reintroduced the wild-type *MST7* and *MST11* genes into ZH32 and yk86, respectively. ZH32C and yk86C were two of the resulting transformants with a single copy of pHZ10 and

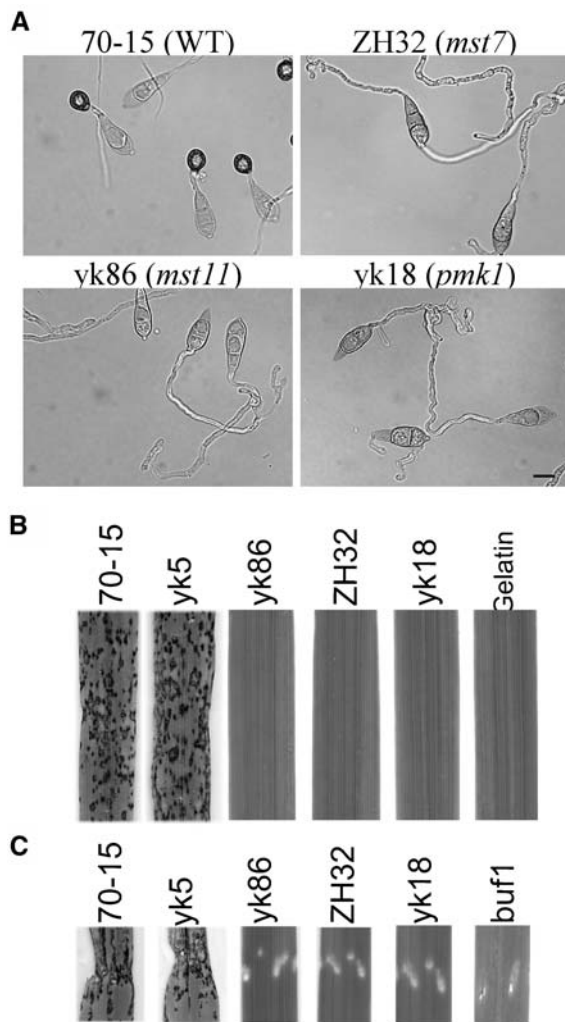


**Figure 3.** *MST7* and *MST11* Were Essential for Appressorium Formation and Plant Infection.

(A) Conidia of the wild-type strain (70-15) and the *mst7* (ZH32), *mst11* (yk86), and *pmk1* (yk18), deletion mutants were incubated on plastic cover slips for 24 h. Whereas 70-15 formed melanized appressoria, the *pmk1*, *mst7*, and *mst11* deletion mutants failed to form appressoria but developed subapical swollen bodies. Bar = 10  $\mu$ m.

(B) Leaves of 2-week-old rice seedling were sprayed with conidia of 70-15, an ectopic transformant yk5, yk86, ZH32, and yk18, and 0.25% gelatin solution.

(C) Rice seedlings were injected with conidia of 70-15, yk5, yk86, ZH32, yk18, and the *buf1* mutant. Whereas 70-15 and yk5 caused lesions on and outside wound sites, all the mutants failed to cause lesions outside the wound site.

pYK21. Each had no obvious defects in appressorium formation (Table 1) or appressorial penetration (data not shown). ZH32C and yk86C were as virulent as the wild-type strain on rice leaves. These data indicate that deletion of the *MST7* or *MST11* gene was directly responsible for defects in appressorium formation and plant infection.

The *mst7* and *mst11* mutants were female sterile but were able to mate as male. However, ectopic transformants such as ZH14 and yk5 obtained from the same transformations were also female sterile. We analyzed 21 random progeny from a cross between ZH32 and Guy11. Eleven progeny were sensitive to hygromycin and normal in appressorium formation and plant infection. In contrast, all 10 hygromycin-resistant progeny failed to form appressoria and infect rice plants. Among 24 random progeny from a cross between yk86 and Guy11, 16 were sensitive to hygromycin and normal in plant infection. Only eight progeny were hygromycin-resistant, but all of them were phenotypically similar to the *mst11* mutant.

#### A Dominant Active *MST7* Allele Partially Rescues the Defects of the *mst11* Deletion Mutant

To further prove that *MST7* and *MST11* activate *PMK1* in *M. grisea*, a putative *MST7* dominant allele was constructed by changing Ser-212 to Asp and Thr-216 to Glu. The resulting *MST7*<sup>S212D T216E</sup> construct pHZ18 was transformed into the *mst11* mutant yk86. Transformants DA5 and DA12 contained a single copy of pHZ18 (data not shown) and were selected for further characterization. Both DA5 (Table 1) and DA12 (data not shown) formed melanized appressoria on hydrophobic surfaces as efficiently as the wild-type strain. However, DA5 (Figure 4A) and DA12 (data not shown) usually produced longer germ tubes before appressorium differentiation. Appressoria formed by DA5 were also smaller than those produced by the wild-type strain (Table 1).

In contrast with 70-15, ~50% of the DA5 germ tubes formed appressoria on the hydrophilic side of GelBond membranes (Figure 4B), indicating that expression of the *MST7*<sup>S212D T216E</sup> allele could bypass the normal surface recognition signal for appressorium formation. DA5 also produced more abundant aerial hyphae than the *mst11* mutant. As a control, we also transformed the wild-type *MST7* gene into yk86 and isolated eight transformants harboring pHZ10, including DAC5 (Table 2). All of them were phenotypically similar to the *mst11* mutant and failed to form appressoria (Figure 4A). These data indicate that the expression of the *MST7*<sup>S212D T216E</sup> allele, but not wild-type *MST7*, partially rescued the defects of the *mst11* deletion mutant in appressorium formation. Therefore, *MST7*<sup>S212D T216E</sup> is a true dominant active allele that is functional without the upstream MEK *MST11*. We also transformed the *MST7*<sup>S212D T216E</sup> construct into the *pmk1* mutant yk18. None of the resulting 12 transformants examined, including transformant DA17, formed appressoria on plastic cover slips or onion epidermal cells (data not shown). No obvious phenotypic differences were observed between DA17 and yk18, indicating that the dominant active *MST7* allele had no function in the *pmk1* mutant. Thus, the MEK encoded by *MST7* likely functions upstream from *PMK1*.

#### Expression of the *MST7*<sup>S212D T216E</sup> Allele Does Not Completely Complement the *mst7* Mutant

The *MST7*<sup>S212D T216E</sup> construct also was introduced into the *mst7* mutant ZH32. Five transformants harboring pHZ18, including DA3-4, were isolated. Similar to DA5, DA3-4 formed melanized

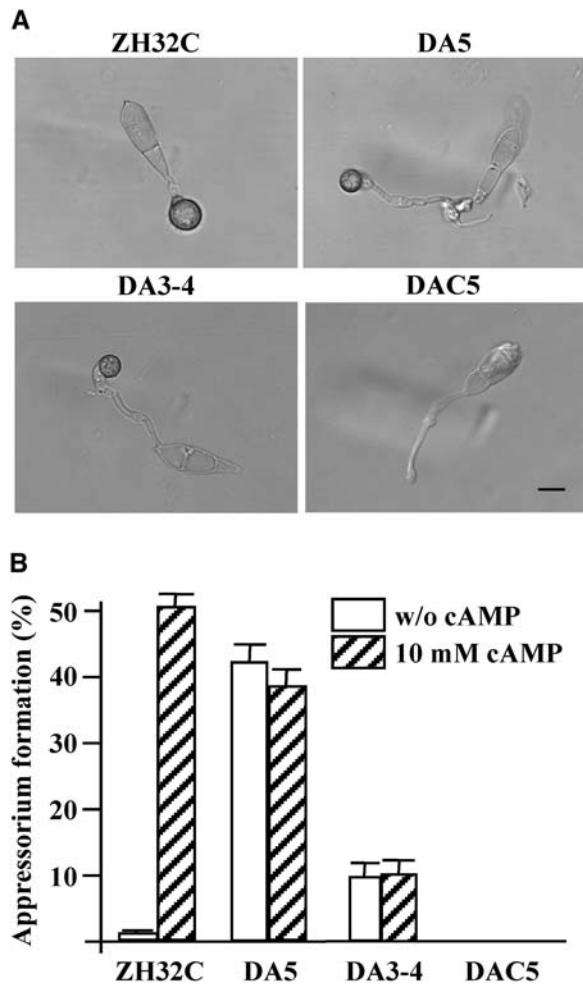


**Figure 4.** Expression of the *MST7*<sup>S212D T216E</sup> Allele in the *mst7* and *mst11* Deletion Mutants.

**(A)** Melanized appressoria formed by transformants ZH32C (*mst7* + *MST7*), DA5 (*mst11* + *MST7*<sup>S212D T216E</sup>), and DA3-4 (*mst7* + *MST7*<sup>S212D T216E</sup>) on the hydrophobic surface of GelBond membranes. Expression of wild-type *MST7* (DAC5) failed to rescue the defect of the *mst11* mutant in appressorium formation. Bar = 10  $\mu$ m.

**(B)** Appressorium formation assays on the hydrophilic surface of Gel-Bond membranes. Transformants DA5 and DA3-4 expressing the *MST7*<sup>S212D T216E</sup> allele formed appressoria by 24 h with or without 10 mM cAMP. Exogenous cAMP stimulated appressorium formation in ZH32C but had no effect in DAC5.

appressoria on both hydrophilic and hydrophobic surfaces. Appressoria produced by DA3-4 also were smaller (Table 1) and were differentiated from longer germ tubes (Figure 4A). However, DA3-4 was less efficient than DA5 and 70-15 in appressorium formation on hydrophobic surfaces (Table 1) or on hydrophilic surfaces with 10 mM cAMP (Figure 4B). By contrast, the complemented transformant ZH32C formed morphologically normal appressoria on hydrophobic surfaces as efficiently as the wild-type strain (Table 1). These data indicated that *MST7*<sup>S212D T216E</sup> was also functional as a dominant active

allele in the *mst7* mutant to stimulate appressorium formation on hydrophilic surfaces. However, the activity of *MST7*<sup>S212D T216E</sup> must be different from that of the wild-type *MST7* gene because appressoria formed by DA5 and DA3-4 were smaller than those formed by the wild-type strain.

Rice infection assays were used to examine the virulence of the *mst7* and *mst11* mutants transformed with the *MST7*<sup>S212D T216E</sup> allele. Although DA5 and DA3-4 formed melanized appressoria (Figure 4), they were nonpathogenic and did not cause lesions on rice leaves in spray infection assays (Figure 5A). On wound-inoculated rice leaves, DA5 and DA3-4 caused expanding lesions similar to those formed by the *buf1* mutant (data not shown). We also assayed appressorial penetration with onion epidermal cells (Figure 5B). The complemented transformants ZH32C and yk86C penetrated and developed infectious hyphae by 48 h. Under the same conditions, no successful penetrations and infectious hyphae were observed in DA5 and DA3-4 (Figure 5B). However, appressoria formed by DA5 and DA3-4 elicited autofluorescence and papilla formation in underlying plant cells (Figure 5B). These phenotypes were similar to those of the *cpkA*, *mps1*, and *pls1* mutants, indicating that appressorial penetration was defective in transformants expressing the *MST7*<sup>S212D T216E</sup> allele. The phenotypic differences between transformants of the *mst7* mutant expressing the wild-type *MST7* or *MST7*<sup>S212D T216E</sup> allele indicated that the S212D and T216E mutations adversely affected the normal functions or activities of *MST7* during appressorial penetration and plant infection.

#### **Pmk1 Is Phosphorylated in Transformants Expressing the *MST7*<sup>S212D T216E</sup> Allele**

To determine whether the Pmk1 MAPK was activated by the dominant active *MST7* allele, we assayed Thr-Gln-Tyr (TEY) residue phosphorylation of Pmk1 with an anti-TpEY specific antibody. Surprisingly, a band that was slightly larger than the expected size of Pmk1 was detected in *pmk1* mutants yk18 (Figure 6) and nn78 (data not shown). Because both Pmk1 (42 kD) and Mps1 (46 kD) MAPKs of *M. grisea* had the TEY phosphorylation site, we generated a *pmk1 mps1* double mutant, DM4 (Table 2). Phenotypically, DM4 had the defects of both the *mps1* (Xu et al., 1998) and *pmk1* deletion mutants (data not shown). In mutant DM4, a band of 42 or 46 kD was not detectable by the anti-TpEY specific antibody (Figure 6), indicating that Mps1 was recognized by the anti-TpEY antibody and responsible for the phosphorylated band observed in yk18. TEY phosphorylation of the Mps1 MAPK was also detectable in vegetative hyphae harvested from complete medium (CM) cultures of 70-15, yk18, and transformant DAC5 (Figure 6). Interestingly, we observed that the level of Mps1 phosphorylation was increased in the vegetative hyphae of yk18 (Figure 6). Phosphorylation of Mps1 also was increased in the vegetative hyphae of the *mst7* and *mst11* mutants (data not shown), indicating that Mps1 activation is stimulated in mutants blocked in the *PMK1* pathway.

In transformant DA5 expressing the *MST7*<sup>S212D T216E</sup> allele, a 42-kD band was detected in proteins isolated from vegetative hyphae (Figure 6). A band of the same size was observed in appressoria of 70-15 (Figure 6) or Guy11 (data not shown). We also detected the same Pmk1 band in appressoria of DA5 on

**Table 2.** Wild-Type and Mutant Strains of *M. grisea* Used in This Study

Strain	Genotype Description	Reference
70-15	Wild-type, <i>MAT1-1</i>	Chao and Ellingboe (1991)
Guy11	Wild-type, <i>MAT1-2</i>	Chao and Ellingboe (1991)
buf1	<i>buf1</i> mutant	Chumley and Valent (1990)
DA128	<i>mac1</i> deletion mutant	Adachi and Hamer (1998)
nn78	<i>pmk1</i> deletion mutant of Guy11, <i>MAT1-2</i>	Xu and Hamer (1996)
JH73	<i>osm1</i> deletion mutant of Guy11, <i>MAT1-2</i>	Dixon et al. (1998)
M3H51	<i>mps1</i> deletion mutant of Guy11, <i>MAT1-2</i>	Xu et al. (1998)
yk18	<i>pmk1</i> deletion mutant of 70-15, <i>MAT1-1</i>	This study
ZH32	<i>mst7</i> deletion mutant of 70-15	This study
ZH14	Ectopic transformant of the <i>MST7</i> knockout construct	This study
ZH32C	ZH32 transformed with pHZ10 (wild-type <i>MST7</i> )	This study
yk86	<i>mst11</i> deletion mutant of 70-15	This study
yk114	<i>mst11</i> deletion mutant of 70-15	This study
yk5	Ectopic transformant of the <i>MST11</i> knockout construct	This study
yk86C	yk86 transformed with the wild-type <i>MST11</i> allele	This study
DA5	<i>MST7</i> <sup>S212D T216E</sup> in yk86	This study
DA12	<i>MST7</i> <sup>S212D T216E</sup> in yk86	This study
DA3-4	<i>MST7</i> <sup>S212D T216E</sup> in ZH32	This study
DA17	<i>MST7</i> <sup>S212D T216E</sup> in yk18	This study
DAC5	Wild-type <i>MST7</i> in yk86	This study
DAC4	Wild-type <i>MST7</i> in yk18	This study
G19	Progeny of Guy11 × yk86, <i>MAT1-1</i>	This study
DP5	<i>mst11 osm1</i> double mutant	This study
DP14	<i>mst11 osm1</i> double mutant	This study
MDS5	<i>MST11</i> <sup>ΔSAM</sup> in yk86	This study
MDR2	<i>MST11</i> <sup>ΔRA</sup> in yk86	This study
DM4	<i>pmk1 mps1</i> double mutant	This study

hydrophobic surfaces (Figure 6). No increase in Pmk1 phosphorylation was observed in DA5 at the appressorium formation stage. Similar results were obtained with mycelia and appressoria of DA3-4 (data not shown). On protein gel blots probed with anti-Pmk1 antibody (Bruno et al., 2004), the Pmk1 band was detectable in all of the samples except the *pmk1* deletion mutant and *pmk1 mps1* double mutant DM4 (Figure 6), indicating that *PMK1* was expressed but not activated in the vegetative hyphae of the wild-type strain and transformants expressing the wild-type *MST7* allele. In transformants expressing the dominant active *MST7* allele, however, TEY phosphorylation and activation of Pmk1 occurred in vegetative hyphae at a level comparable with that of the appressorium formation stage (Figure 6). These data further confirm that *PMK1* functions downstream from *MST7*.

#### The Intracellular cAMP Level Is Reduced in Transformants Expressing the *MST7*<sup>S212D T216E</sup> Allele

We measured the intracellular cAMP levels in the mutants defective in the *PMK1* pathway (Table 3). The *pmk1*, *mst7*, and *mst11* deletion mutants had intracellular cAMP levels comparable with that of the wild-type strain (Table 3), suggesting that deletion of *PMK1*, *MST7*, or *MST11* did not have significant effects on the cAMP signaling pathway. However, in transformants DA5 and DA3-4 expressing the *MST7*<sup>S212D T216E</sup> allele, the intracellular cAMP level was significantly lower than that of the

wild-type strain 70-15 (Table 3) but higher than that of the *mac1* mutant with the adenylate cyclase gene deleted (Adachi and Hamer, 1998). Therefore, expression of the *MST7*<sup>S212D T216E</sup> allele likely had a negative effect on the cAMP signaling pathway. Because the cAMP signaling pathway is known to regulate surface recognition (Mitchell and Dean, 1995), it is possible that activation of the Pmk1 MAPK is involved in the downregulation of cAMP signaling after initiating appressorium formation.

#### The SAM Domain Is Essential for the Activity of *MST11*

To determine the function of the SAM and RA domains, we generated *MST11* mutant alleles with amino acid residues 62 to 160 and 257 to 353 deleted (Figure 7A). The *MST11*<sup>ΔSAM</sup> (pYK39) and *MST11*<sup>ΔRA</sup> (pYK45) constructs were transformed into the *mst11* deletion mutant yk86. MDS5 and MDR2 (Table 2) were two of the resulting zeocin-resistant transformants containing a single copy of pYK39 and pYK45, respectively. On rice leaves sprayed with conidia from yk86C and MDR2, numerous lesions were observed at 7 d after inoculation. Under the same conditions, MDS5 failed to cause any lesions on rice leaves (Figure 7B). When assayed for appressorium formation on hydrophobic surfaces, yk86C and MDR2 produced melanized appressoria (Figure 7C). However, MDS5 and other transformants expressing the *MST11*<sup>ΔSAM</sup> allele failed to form appressoria. Only subapical swollen bodies similar to those of the *mst11* mutant were observed in MDS5 (Figure 7C). On the epidermal cells of rice

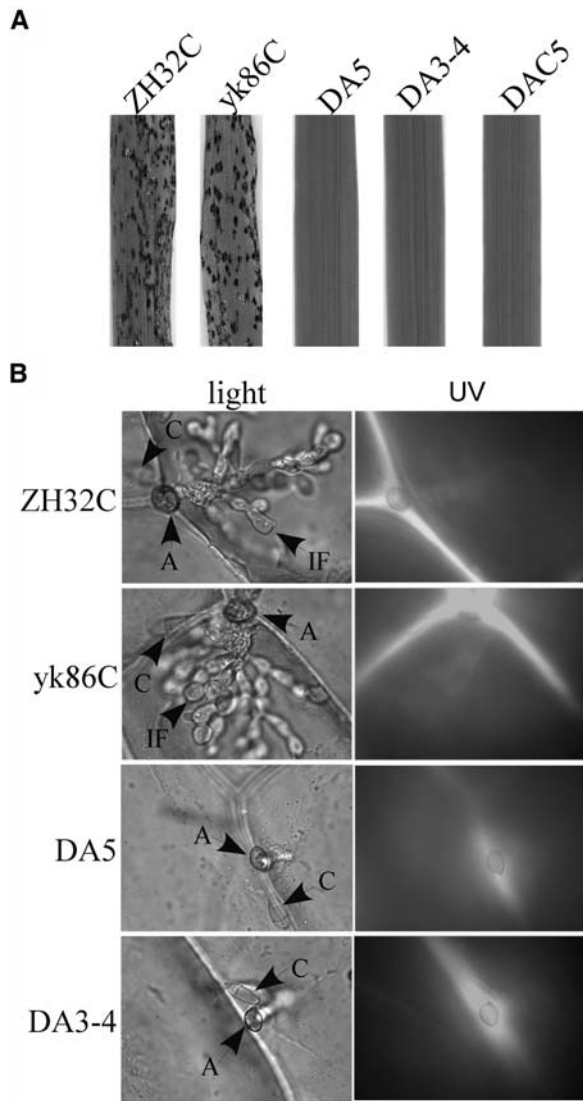


**Figure 5.** Plant Infection and Appressorial Penetration Assays with Transformants Expressing the Dominant Active *MST7* Allele.

**(A)** Rice leaves sprayed with conidia from ZH32C (*mst7* + *MST7*), yk86C (*mst11* + *MST11*), DA5 (*mst11* + *MST7*<sup>S212D T216E</sup>), DA3-4 (*mst7* + *MST7*<sup>S212D T216E</sup>), and DAC5 (*mst11* + *MST7*).

**(B)** Penetration assays with onion epidermi examined under DIC (left panels) and epifluorescence (right panels) microscopy. Appressoria formed by ZH32C and yk86C penetrated and differentiated infectious hyphae at 48 h. DA5 and DA3-4 failed to penetrate onion epidermal cells but elicited autofluorescence and papilla formation in underlying plant cells. A, appressorium; C, conidium; IF, infectious hypha.

leaf sheaths, MDR2 but not MDS5 formed appressoria, penetrated, and developed infectious hyphae (Figure 7C). These data indicated that the SAM domain was essential for the regulatory functions of *MST11* in appressorium formation and plant infection. By contrast, the RA domain was dispensable because the *MST11*<sup>ΔRA</sup> allele complemented the defect of the *mst11*

deletion mutant in appressorium formation and plant infection (Figure 7).

#### Both *Mst11* and *Mst7* Interact with the Putative Adaptor Protein *Mst50*

In *S. cerevisiae*, Fus3 and Kss1 directly interact with several other components of the pheromone response pathway, including Ste7 and Ste11 (Kranz et al., 1994; Kusari et al., 2004). To assay direct interactions of Pmk1 with *Mst7* or *Mst11*, we constructed Pmk1 as the bait and *Mst7* and *Mst11* as the preys with the Stratagene HybridZapII yeast two-hybrid assay system. No direct interaction was observed between Pmk1 and *Mst7* or Pmk1 and *Mst11* (Figure 8). We also conducted yeast two-hybrid assays with Pmk1 as the prey and *Mst7* or *Mst11* as the bait and failed to detect direct interaction between them (data not shown). However, a very weak interaction between *Mst7* and *Mst11* was detectable in repeated yeast two-hybrid assays (Figure 8).

*MST11* contains an N-terminal SAM domain, which is known to be involved in interactions with other proteins with SAM domains. In the *M. grisea* genome, predicted ORF MG05199 (named *MST50*) was homologous with yeast Ste50 (Ramezani-Rad, 2003) and *U. maydis* Ubc2. *MST50* contained an N-terminal SAM domain that was highly homologous with the SAM domain of *MST11*. In yeast two-hybrid assays, *Mst50* strongly interacted with *Mst11* (Figure 8). It also interacted with *Mst7*, but its interaction with *Mst7* was weaker than that with *Mst11* (Figure 8). However, there was no detectable interaction between *Mst50* and Pmk1 (Figure 8). These data indicate that *Mst50* directly interacts with both *Mst11* and *Mst7*. The association of *Mst11* and *Mst7* with *Mst50* may result in the formation of a protein complex and stabilize the *Mst11*–*Mst7* interaction. Therefore,

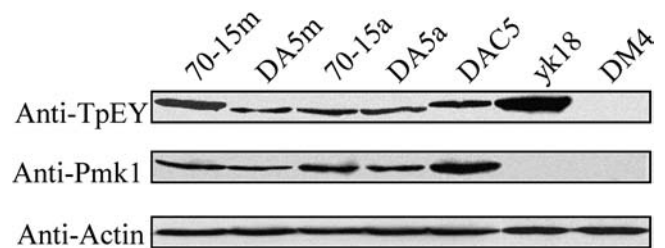


**Figure 6.** Protein Gel Blot Analysis of the Expression and Activation of Pmk1.

Total proteins were isolated from mycelia (70-15m) and appressoria (70-15a) of the wild-type strain 70-15, mycelia (DA5m) and appressoria (DA5a) of DA5 expressing the *MST7*<sup>S212D T216E</sup> allele, mycelia of DAC5 (*mst11*+*MST7*), *pmk1* deletion mutant yk18, and *pmk1 mps1* double mutant DM4. When probed with an anti-TpEY antibody (top panel), a 42-kD band was detected in appressoria of 70-15, and mycelia or appressoria of DA5. In mycelia of 70-15, DAC5 and yk18, a band slightly bigger than the Pmk1 band was detectable. In DM4, TEY phosphorylation of Pmk1 or Mps1 was not observed. When probed with an anti-Pmk1 antiserum (middle panel), a 42-kD Pmk1 band was detected in all the samples except yk18 and DM4. The bottom panel was detection with an anti-Actin antibody to show similar amount of total protein was loaded in each lane.

**Table 3.** Measurement of Intracellular cAMP Levels in Mycelia

Strain	fmol of cAMP/mg of Mycelia <sup>a</sup>	Percentage of 70-15 (Wild Type)
70-15	885.3 ± 65.7 <sup>b</sup>	100.0
yk18	804.8 ± 63.9	90.9
ZH32	689.1 ± 61.6	77.8
yk86	898.6 ± 86.3	101.5
DA5	470.5 ± 39.3	53.1
DA3-4	339.2 ± 33.6	38.3
DA128	99.9 ± 11.2	11.3

<sup>a</sup> Lyophilized weights of mycelia.

<sup>b</sup> Means and standard deviations were calculated from at least three independent experiments.

Mst50 may function as an adaptor protein for the upstream components of the *PMK1-MST7-MST11* cascade.

### The *PMK1* Pathway Regulates Certain Osmoregulation Processes Independent of *OSM1*

The *pmk1*, *mst7*, and *mst11* mutants grew slower than the wild-type strain on oatmeal agar plates with 1 M sorbitol (Table 1). To determine whether enhanced sensitivity of these mutants to osmotic stresses was related to the *OSM1* pathway, we crossed yk86 with *osm1* mutant JH73 (Dixon et al., 1999). Two *mst11 osm1* progeny, DP5 and DP14, were isolated and confirmed by DNA gel blot analyses. Similar to the *mst11* mutant, the *mst11 osm1* double mutants were defective in appressorium formation and plant infection (data not shown). However, the *mst11 osm1* double mutants were more sensitive to osmotic stresses than the *osm1* mutant and failed to grow on CM media with 1 M sorbitol (Figure 9A), even after prolonged incubation for 2 weeks (Figure 9B). On hydrophobic surfaces, appressorium formation but not conidium germination was blocked in the *osm1* mutant by 1 M sorbitol (Figure 9C). In the *osm1 pmk1* double mutant, however, conidium germination was severely inhibited by 1 M sorbitol (Figure 9C) or 1.4 M NaCl. Therefore, the *PMK1* pathway may regulate certain osmoregulation responses independent of *OSM1* in *M. grisea* during vegetative growth or conidium germination. We also observed that the *mst11* mutant was more sensitive to osmotic stresses than the *pmk1* and *mst7* mutants (Table 1). Expression of the dominant active *MST7* allele rescued the growth defect of the *mst7* mutant but not the *mst11* mutant on oatmeal agar plates with 1 M sorbitol (Table 1). These data indicate that Mst11 but not Mst7 may be involved in the Osm1 pathway in response to osmotic stresses, similar to the role played by Ste11 in the yeast HOG1 pathway (Ramezani-Rad, 2003).

## DISCUSSION

In the *M. grisea* genome sequence, there are three MEKKs, three MEKs, and three MAPKs. The *PMK1*, *MPS1*, and *OSM1* MAPK genes, which are homologous with yeast *FUS3/KSS1*, *SLT2*, and *HOG1* (Gustin et al., 1998; Dohman, 2002), respectively, have

been shown to regulate appressorium formation, cell wall integrity, and osmoregulation in *M. grisea*. In addition to *MST7* and *MST11*, which were characterized in this study, we have identified putative MEK genes *MgMMK2* (MG06482) and *MgPBS2* (MG10268), which are homologous with yeast *MMK1/MMK2* and *PBS2*, and putative MEKK genes *MgBCK1* (MG00883) and *MgSSK2* (MG00183), which are homologous with yeast *BCK1* and *SSK2*. Preliminary data indicated that mutants with *MgMMK2* or *MgSSK2* deleted were phenotypically similar to the *mps1* mutant (Xu et al., 1998) and defective in appressorial penetration, whereas mutants with *MgPBS2* or *MgBCK1* deleted were similar to the *osm1* mutant (Dixon et al., 1999) and sensitive to hyperosmotic stresses (J.-R. Xu, unpublished data). Therefore, it is likely that *M. grisea* has the following three MAPK

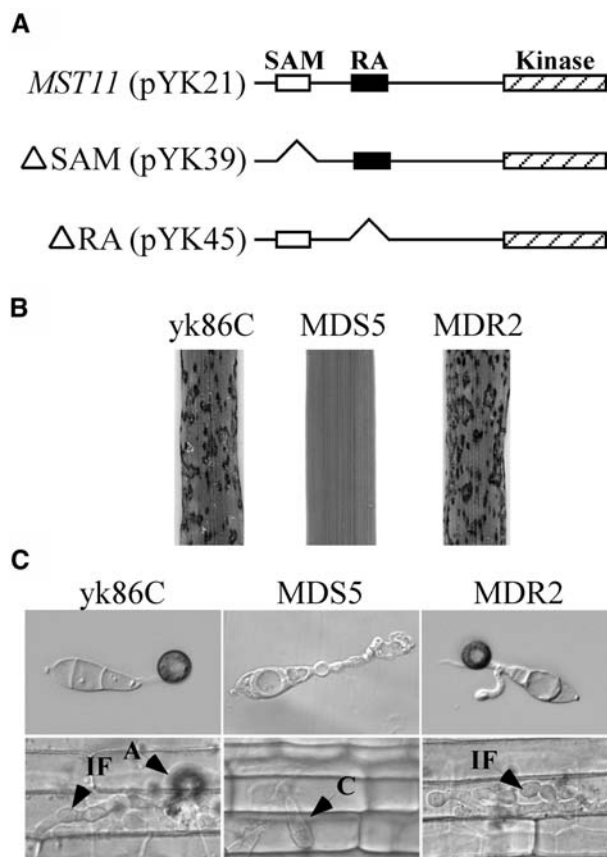


**Figure 7.** Functional Characterization of the SAM and RA Domains of *MST11*.

(A) Amino acid residues containing the SAM and RA domains were deleted in the  $\Delta$ SAM construct pYK39 and the  $\Delta$ RA construct pYK45. Both pYK39 and pYK45 had the same native *MST11* promoter and terminator sequences as the *MST11* complementation vector pYK21.

(B) Rice leaves sprayed with conidia from transformants of yk86C expressing pYK21 (yk86C), pYK39 (MDS5), or pYK45 (MDR2).

(C) Appressorium formation assays on plastic cover slips (top panels) and penetration assays on epidermal cells of rice leaf sheaths (bottom panels) with yk86C, MDS5, and MDR2. Transformants yk86C and MDR2 but not MDS4 formed appressoria and penetrated rice leaf sheath cells. A, appressorium; C, conidium; IF, infectious hypha.

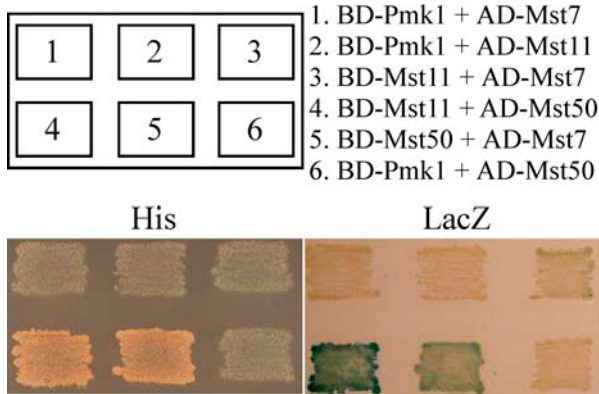


**Figure 8.** Yeast Two-Hybrid Assays of the Interactions between Pairs of *PMK1*, *MST7*, *MST11*, and *MST50*.

Yeast transformants containing the bait and prey constructs of *PMK1*, *MST7*, *MST11*, and *MST50* as indicated (top panels) were patched on SD-Leu-Trp-His plates (bottom left, His). BD- and AC- stand for clones generated in pBD-GAL4 and pAD-GAL4, respectively. Colony growth was examined after 48 h incubation. The same set of yeast strains were grown on nitrocellulose membranes placed on the SD-Leu-Trp plates and assayed for  $\beta$ -galactosidase activities (bottom right, LacZ).

cascades: *MST11-MST7-PMK1*, *MgBCK1-MgMMK2-MPS1*, and *MgSSK2-MgPBS2-OSM1*. Similar components of these cascades were identified in the *N. crassa* and *F. graminearum* genomes.

*MST11*, similar to *kpp4* and other *STE11* homologs, has the SAM domain at the N terminus (Muller et al., 2003; Grimshaw et al., 2004). The originally published *N. crassa* *NRC-1* sequence (Kothe and Free, 1998) was shorter than its actual genomic sequence (NCU06182) and lacked the SAM domain. In the *M. grisea* genome, two other proteins contain the SAM domain. One is the *STE50* homolog (*MST50*). The other is the predicted ORF MG06334, which shares no homology with *MST50* or *MST11* outside of the SAM domain. Its homolog in yeast (*VTS1*) is involved in RNA degradation. *MST11* and its homologs from *N. crassa* and *F. graminearum* all have a RA domain downstream from the SAM domain. Two Ras homologs in *M. grisea* (*MgRas1* and *MgRas2*) are homologous with yeast *Ras1* and *Ras2*. Our preliminary studies indicated that both *MgRas1* and *MgRas2* interact with *MST11* in yeast two-hybrid assays. Because Ras proteins are known to function upstream of MAPK cascades (Liebmann, 2001; Cherkasova et al., 2003), it is possible that *MST11* is activated by Ras proteins in *M. grisea*. In *S. cerevisiae*, the PAK kinase *STE20* is essential for *Ste11* activation and the mating and filamentous growth pathways (Bardwell, 2004). By contrast, both *CHM1* and *MST20*, the only PAK kinase-encoding genes in *M. grisea*, are dispensable for appressorium formation and possibly not involved in activating the *PMK1* MAPK pathway (Li et al., 2004). Therefore, the upstream components activating the *MST11-MST7-PMK1* cascade in *M. grisea* are different from those of the pheromone response and filamentation pathways in *S. cerevisiae*. In the fission yeast *Schizosaccharomyces pombe*, the sexual response MAPK pathway is regulated by both trimeric G-proteins and *Ras1* (Xu et al., 1994; Papadaki et al., 2002). The

*PMK1* MAPK cascade may be regulated by similar mechanisms in *M. grisea*.

In *U. maydis*, the *Fuz7/Ubc5* MEK and *Kpp4/Ubc4* both are required for transcriptional responses to pheromone, filamentous growth, mating, and pathogenicity (Banuett and Herskowitz, 1994; Andrews et al., 2000; Muller et al., 2003). However, unlike *M. grisea*, *U. maydis* has at least two MAPK genes, *Kpp2* and *Kpp6*, that function downstream from *Ubc4* and *Fuz7* (Andrews et al., 2000; Muller et al., 2003). In the human pathogen *Candida albicans*, *HST7* MEK and *CEK1* MAPK are involved in yeast-hyphal transition, fungal pathogenesis, and mating responses

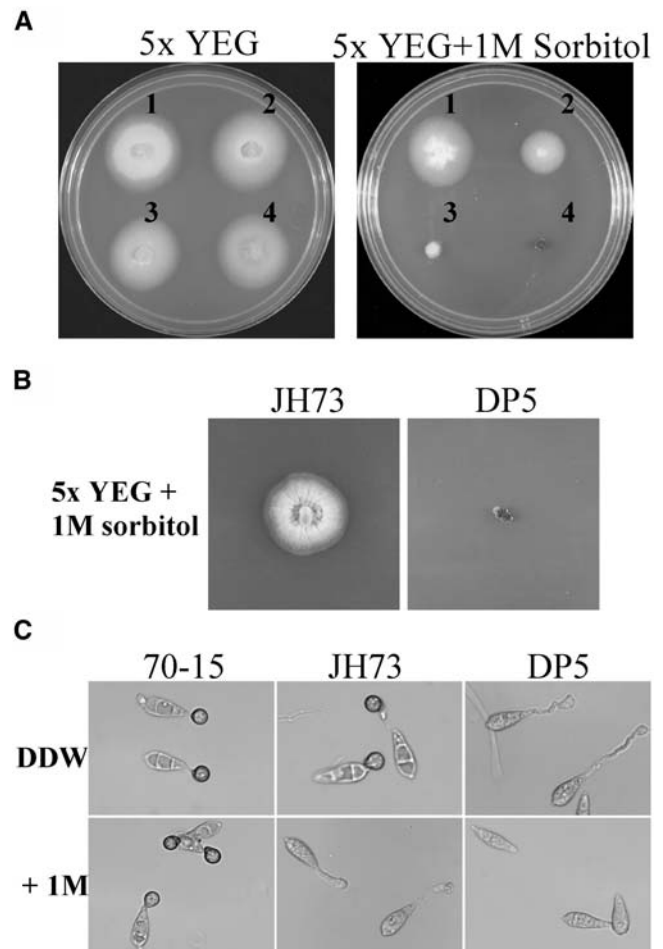


**Figure 9.** Sensitivity of the *mst11 osm1* Double Mutant to Osmotic Stresses.

(A) Colony growth on 5 $\times$  YEG or 5 $\times$  YEG + 1 M sorbitol plates. Strains 1 to 4 were the wild-type strain 70-15, the *mst11* deletion mutant yk86, the *osm1* mutant JH73, and the *mst11 osm1* double mutant DP5, respectively. Photos were taken after incubation at 25 $^{\circ}$ C for 5 d.

(B) Colonies of JH73 (*osm1*) and DP5 (*mst11 osm1*) grew on 5 $\times$  YEG + 1 M sorbitol plates for 2 weeks. No significant growth was observed in DP5.

(C) Conidia of 70-15 and the *osm1* and *mst11 osm1* double mutants were incubated on plastic cover slips for 24 h in DDW (top panels) or in 1 M sorbitol (bottom panels).

(Kohler and Fink, 1996; Csank et al., 1998; Chen et al., 2002). By contrast, homologs of Fus3/Kss1, Ste7, and Ste11 in the basidiomycete *Cryptococcus neoformans* are required only for mating and cell type-specific differentiation but do not play important roles in virulence (Clarke et al., 2001). In *N. crassa*, the *nrc-1* ascospores have a flattened appearance and are not viable (Kothe and Free, 1998). In *M. grisea*, *mst11* mutants were female sterile but male fertile. Although ascospore viability may be reduced in the *mst11* mutant, *mst11* progeny were viable.

Surprisingly, no direct interaction was detected between Pmk1 and Mst7. It is possible that the Pmk1–Mst7 interaction is too weak or too transient to be detected by yeast two-hybrid assays or that only phosphorylated Mst7 will interact with its downstream target Pmk1. We also failed to detect physical interactions between Pmk1 and Mst11 or Mst50. Interestingly, Mst7 has a putative MAPK docking site (residues 12 to 20) that is conserved among its homologs from other filamentous fungi. Our preliminary data indicate that this putative docking site is essential for *MST7* to complement defects of the *mst7* mutant (X. Zhao and J.-R. Xu, unpublished data). Therefore, it is likely that Mst7 interacts with Pmk1 via this MAPK docking site in *M. grisea* but that this interaction may be too transient or too weak to be detected by two-hybrid assays. In *S. cerevisiae*, Ste5 is the scaffold protein that interacts with different components of the pheromone response pathway. In the *M. grisea* genome, MG00134 is weakly homologous with Ste5, but their homology is limited to the Ring-finger domain. Our preliminary data indicated that mutants with MG00134 deleted had no obvious defect in infection-related morphogenesis (G. Park and J.-R. Xu, unpublished data). The Mst11, Mst7, and Pmk1 proteins also lack homology with their yeast counterparts in the regions that are involved in interaction with Ste5. In *U. maydis*, Ubc2 interacts with Ubc4 via its N-terminal SAM domain (Mayorga and Gold, 2001). Ubc2 contains two C-terminal Src homology 3 domains that are likely to be involved in protein–protein interactions. Mst50, the *M. grisea* homolog of Ubc2, has the SAM and RA domains but lacks the Src homology 3 domains. Mst50 interacted with Mst11 and Mst7 but not with Pmk1 in yeast two-hybrid assays (Figure 8). We have generated the *mst50* gene replacement mutant. Preliminary data indicated that the *mst50* mutant was phenotypically similar to the *mst11* mutant and was defective in appressorium formation and plant infection. Expression of the dominant *MST7* allele also rescued the defects of the *mst50* mutant in appressorium formation (G. Park and J.-R. Xu, unpublished data). Therefore, *MST50* functions as an upstream component of the *PMK1* MAPK pathway in *M. grisea*. However, it remains possible that *MST50* also is involved in other signaling pathways. To further prove that *MST7* activates *PMK1*, we generated the *PMK1*<sup>D59N</sup>, *PMK1*<sup>D231N</sup>, and *PMK1*<sup>D59N D231N</sup> mutant alleles, which were equivalent to *FUS3*<sup>D48N</sup> and *FUS3*<sup>D227N</sup> (Brill et al., 1994). However, preliminary data indicated that the D48N and/or D227N mutations of *PMK1* had no gain-of-function effects in *M. grisea*.

The anti-TpEY antibody from Cell Signaling Technology detected both Pmk1 and Mps1 in *M. grisea* (Figure 6). Because the size difference between Pmk1 and Mps1 is only 4 kD, it was impossible to observe two distinct bands. We tried the Anti-ACTIVE MAPK polyclonal antibody from Promega (catalog

number V8031; Madison, WI) and found that it also detected the phosphorylation of both Pmk1 and Mps1 in *M. grisea*. Interestingly, the level of Mps1 phosphorylation was increased in the vegetative hyphae of the *pmk1* mutant (Figure 6). However, phosphorylation of Pmk1 was not detectable in the vegetative hyphae of the *mps1* mutant (data not shown) or 70-15 (Figure 6). These data suggest that Mps1 may be overactivated to compensate for the cell wall defects associated with the *pmk1* mutant during vegetative growth, but the level of Pmk1 activation is not changed in the *mps1* mutant. In transformants expressing the dominant active *MST7* allele or in the wild-type strain during appressorium formation, however, the phosphorylation of Mps1 was repressed (Figure 6). These data indicate that there is cross talk between the *PMK1* and *MPS1* pathways and that the activation of Pmk1 may have a negative effect on Mps1 phosphorylation. It will be important to determine the molecular mechanisms involved in the interactions between the Pmk1 and Mps1 MAPK pathways. Although the *pmk1*, *mst7*, and *mst11* mutants had weakened cell walls (see Supplemental Figure 1 online), they produced more conidia and aerial hyphae than the *mps1* mutant. Colonies formed by these mutants did not display the autolysis phenotype observed in the *mps1* mutant (Xu et al.,

**Table 4.** PCR Primers Used in This Study

Name	Sequence (5' → 3')
HPF	TGCACCACCCGTACTTCG
HPR	CGATCGATGTGGGTTGCTGTCCAACATATGGGT
1F	ATAAGGATCCTACCCCTTACTGTACGAGCT
2R	AATAGGCCGCGCTCCTGGTACAAGCTGTTA
3F	ATAAGGCCGCGCCTTCTCACTACCTATGCGA
4R	AATAAAGCTTAAGCGTGTCCGATACTAA
5F	GAAGCGCATTGTGCGAGAACTA
6R	CACCTTCTGAATCATATCCTCGA
7F	AATAGCGGCCGCGAGCTAGGCTAGAAGTGG A
H8F	GAACCTTATAACGACATAGCCGATGAGTTTGTCCGGCACT
H9R	AGTGCCGACAAACTCATCGGCTATGTCGTTAATAAGTTTC
S1F	CCATCGATTCCGTCGAGTCCTTGC
S1R	CCAAGCTTCTGCAGTGCCAGACAG
S2F	AACTGCAGTGCAGGGTTCCGGTGTTC
S2R	CGACTAGTCCAATATTAGTTAGTGCT
S3F	TGGGAGAGAATTGGGATA
S3R	ATCCCTGTCCGATGAGTG
S4F	ACCACCTTCGCACATAG
S4R	GAAACACGGGGTATCTCC
SDF1	CCCAAGCTTTCTAGCAGCCGTGTCATG
SDR1	CCCAAGCTTGTGAATCATGATCATCG
RDF1	CCATCGATGAGCCAGGACAGCTGAG
RDR1	CCATCGATGGCAGCCATCAGCGATCC
F9	GATCGGAATTCATGAGCTTCAACACGGGGACGGCGTA
R10	GATCCTGCAGTCATATTATTCCTCCTGGGGGATC
M11F6	CCGAATTCATGGCCATGTTGGCTTCA
M11R7	CTACCCGGGTTACGTGATAGGAGTCAGGAAG
ADF	ATAAGGATCCATGGCCGACCCGTTTGCGCCGCGACCCAT
ADR	AATAAGATCTCTAGAAACCATAACTCCCAGTCGATG
BDF	ATAAGAGCTCATGGCCGACCCGTTTGCGCCGCGACCCAT
BDR	AATAGACGTGCGCTAGAAACCATAACTCCCAGTCGATG
PF1	GAGAATTCATGTCTCGCGCCAAATCCA
PR2	TAACCCGGGCTTACCGCATAATTTCTCTG
PR3	GATCTCGAGTTACCGCATAATTTCTCTG

1998), indicating that mutants blocked in the Pmk1 or Mps1 pathway may have different cell wall defects.

The other interesting phenomenon we observed was that expression of the *MST7*<sup>S212D T216E</sup> allele rescued the defect in appressorium formation but not plant infection in the *mst7* or *mst11* deletion mutant. One possible explanation is that Pmk1 is activated during appressorium formation but Pmk1 activity has to be downregulated before penetration. Activation of Pmk1 by constitutively active Mst7 will likely block penetration by interfering with the normal fluctuation of *PMK1* activity during plant infection. The other possibility is that *PMK1* only regulates appressorium formation but not infectious hyphal growth. However, that is unlikely because previous studies of several fungal pathogens have indicated that mutants with *PMK1* deleted or its homologs are nonpathogenic and fail to infect through wounds (Xu and Hamer, 1996; Takano et al., 2000; Zheng et al., 2000; Di Pietro et al., 2001; Ruiz-Roldan et al., 2001). Because the activation of Pmk1 suppressed the phosphorylation of Mps1, it is also possible that constitutively active *MST7* blocks the *MPS1* MAPK pathway, which is required for appressorial penetration in *M. grisea* (Xu et al., 1998). An alternative explanation is that these transformants expressing the *MST7*<sup>S212D T216E</sup> allele may have defects in the cAMP signaling pathway that regulates surface recognition and appressorial turgor generation in *M. grisea* (Xu et al., 1997; Thines et al., 2000). Similar to the *cpkA* mutant, appressoria formed by DA5 and DA3-4 were smaller than those of the wild-type strain. In addition, DA5 and DA3-4 had reduced intracellular cAMP levels (Table 3). In yeast and several fungal pathogens, cAMP signaling is intimately associated with a MAPK homologous with *PMK1* for regulating various developmental and plant infection processes (Cherkasova et al., 2003; Kaffarnik et al., 2003; Lee et al., 2003). Further characterization of transformants DA5 and DA3-4 will be helpful in understanding the relationship between the cAMP signaling and *PMK1* MAPK pathways in *M. grisea*.

## METHODS

### Culture Conditions and Plant Infection Assays

Wild-type *Magnaporthe grisea* strains Guy11 and 70-15 (Chao and Ellingboe, 1991) and all related mutants (Table 2) were cultured on oatmeal agar plates at 25°C. To generate the *pmk1 mps1* double mutant, the *MPS1* gene replacement vector pM3H22 (Xu et al., 1998) was introduced into the *pmk1* mutant nn78 by cotransformation with the bleomycin resistance vector pAC905 (Zheng et al., 2000). Media were supplemented with 250 µg/mL hygromycin B (Calbiochem, La Jolla, CA) or 100 µg/mL zeocin (Invitrogen, Carlsbad, CA) for selection of hygromycin-resistant or zeocin-resistant transformants, respectively. Monoconidial culture isolation, genetic crosses, penetration assays, and growth rate measurements were performed as described previously (Li et al., 2004; Park et al., 2004). Appressorium formation was assayed on plastic microscope cover slips (Fisher Scientific, Pittsburgh, PA) or GelBond membranes (Cambrex, East Rutherford, NJ). Vegetative hyphae harvested from 2-d-old CM cultures were tested for cell wall defects as described (Xu et al., 1998) with 2.5 mg/mL lysing enzymes (Sigma-Aldrich, St. Louis, MO). Conidia were resuspended in 10 mM cAMP to test cAMP responsiveness. Two-week-old seedlings of the rice (*Oryza sativa*) cv Nipponbare and 8-d-old seedlings of the barley (*Hordeum vulgare*) cv

Golden Promise were used for spray or injection infection assays (Park et al., 2004).

### Molecular Manipulations

Standard molecular biology procedures were followed for RNA gel blot, protein gel blot, and DNA gel blot analyses and enzymatic manipulations with DNA and RNA. Proteins were extracted from mycelia collected from 2-d-old CM cultures and appressoria formed on plastic Petri plates for 12 h as described previously (Bruno et al., 2004). Total proteins (~20 µg) were separated on a 12% SDS-PAGE gel and transferred to nitrocellulose membranes. Antigen-antibody detection was performed with the ECL Supersignal system (Pierce, Rockford, IL). The anti-Pmk1 antiserum (Bruno et al., 2004) was used to detect Pmk1 expression. TEY phosphorylation of MAPKs was detected with the PhosphoPlus p44/42 MAPK antibody kit (Cell Signaling Technology, Beverly, MA) according to the manufacturer's instructions. A monoclonal anti-actin antibody (Sigma-Aldrich) was used to detect actin.

### *MST11* Gene Replacement Vectors and Mutants

To generate the *MST11* gene replacement vector, the *hph* gene was amplified with primers HPF and HPR (Table 4) and cloned into the *EcoRI* site of pBluescript II KS- (Stratagene, La Jolla, CA) as pGP18. A 1.2-kb fragment of *MST11* was amplified with S1F and S1R and cloned between the *Clal* and *HindIII* sites on pGP18 as pYK15. A 0.7-kb fragment downstream from *MST11* was amplified with primers S2F and S2R and cloned between *PstI* and *SpeI* sites on pYK15 as the *MST11* gene replacement vector pYK16. The complementation vector pYK21 was constructed by cloning a 4.2-kb fragment of *MST11* amplified with primers S1F and S2R between the *Clal* and *SpeI* sites of pYK11. In pYK11, the bleomycin resistance gene amplified from pAC905 was cloned into the *XmnI* site on pBC KS+ (Stratagene). To generate the *MST11*<sup>ΔSAM</sup> allele, a 1.3-kb fragment of *MST11* amplified with primers S1F and SDR1 was cloned between the *Clal* and *HindIII* sites on pYK11 as pYK38. A 2.6-kb downstream fragment was amplified with primers SDF1 and S2R and cloned between the *HindIII* and *SpeI* sites of pYK38 as pYK39 (Figure 8). To generate the *MST11*<sup>ΔRA</sup> allele, a 1.9-kb fragment amplified with primers S1F and RDR1 was cloned into the *Clal* site on pYK11 as pYK27. A 2.2-kb downstream fragment of *MST11* was amplified with primers RDF1 and S2R and cloned in pYK27 as pYK45 (Figure 8).

### *MST7* Gene Replacement Vectors and Mutants

Approximately 800-bp upstream and downstream flanking sequences of *MST7* were amplified with primers 1F and 2R, and 3F and 4R, respectively (Figure 2). The resulting PCR products were digested with *FseI* and *AscI* and ligated with the *hph* cassette released from pCX63 (Zhao et al., 2004). The *MST7* gene replacement construct was amplified with primers 1F and 4R using the ligation product as the template and directly transformed into 70-15 as described previously (Zhao et al., 2004). One *mst7* gene replacement mutant was identified by screening hygromycin-resistant transformants with primers 5F and 6R and confirmed by DNA gel blot analysis. The complementation construct pHZ10 was generated by cloning the full-length *MST7* gene amplified with primers 7F and 8R between the *NotI* and *HindIII* sites on pYK11. Primers H8F and H9R were used to introduce the S212D and T216E mutations of *MST7* on pHZ10 with the Quickchange II site-direct mutagenesis kit (Stratagene). The resulting vector, pHZ18, was sequenced to confirm the S212D and T216E mutations, which were equivalent to the S259D and T263D mutations of *Ustilago maydis fuz7* (Muller et al., 2003) and the S217E and S221E mutations of constitutively active MEKs (Cowley et al., 1994).

### Yeast Two-Hybrid Assays

The HybridZap2.1 yeast two-hybrid system (Stratagene) was used to assay protein-protein interactions. The ORFs of *PMK1* and *MST11* were amplified from first-strand cDNA of 70-15 with primers PF1/PR2 and M11F6/M11R7 and cloned between the *EcoRI* and *SmaI* sites on pBD-GAL4 as the bait constructs pCX38 and pGP80, respectively. The prey constructs of *PMK1* and *MST11* were constructed by cloning PCR products amplified with primers PF1/PR3 and M11F6/M11R8 into pAD-GAL4-2.1. The *MST50* ORF was amplified with primers F9 and R10, digested with *EcoRI* and *PstI*, and cloned into pBD-GAL4 as the bait vector pCX85 and into pAD-GAL4-2.1 as the prey vector pGP88. The *MST7* ORF was amplified with primers ADF and ADR and cloned in pAD-GAL4 as the prey construct pHZ15. The *MST7* ORF also was amplified with primers BDF and BDR and cloned in pBD-GAL4 as the bait construct. The resulting bait and prey vectors were cotransformed in pairs into yeast strain YRG-2 (Stratagene) with the alkali-cation yeast transformation kit (BIO 101, Carlsbad, CA). The Leu<sup>+</sup> and Trp<sup>+</sup> transformants were isolated and assayed for growth on SD-Trp-Leu-His medium. The expression of the LacZ reporter gene was assayed with a solution containing an X-Gal substrate according to the instructions provided by Stratagene.

### Intracellular cAMP Measurements

Mycelia were collected from 2-d-old CM liquid cultures by filtering through Miracloth and frozen in liquid nitrogen. All fungal samples were lyophilized for 16 h and weighed. For every 100 mg of mycelia, 1 mL of ice-cold 6% (w/v) trichloroacetic acid was added (Nishimura et al., 2003). Mycelia were then ground to a powder and centrifuged in Eppendorf tubes at 14,000 rpm for 2 min at 4°C. The supernatant (200  $\mu$ L) was transferred to a new tube and extracted five times with an equal volume of chloroform. The concentration of cAMP was determined with the cAMP enzyme immunoassay system (Amersham-Pharmacia Biotech, Uppsala, Sweden) according to the manufacturer's instructions.

Sequence data from this article have been deposited with the EMBL/GenBank data libraries under accession numbers EAA49142 for *MST7*, EAA56368 for *MST11*, EAA52507 for *MST50* (MG05199), EAA56363 for the SAM domain protein MG06334, EAA56511 for *MgMMK2* (MG06482), EAA48205 for *MgPBS2* (MG10268), EAA49225 for *MgBCK1* (MG00883), EAA48525 for *MgSSK2* (MG00183), P23561 for *S. cerevisiae* Ste11, P28829 for *S. pombe* Byr2, AAG30205 for *C. neoformans* CnSte11, AAN63948 for *U. maydis* Kpp4, CAD44493 for *Aspergillus nidulans* SteC, AAG30572 for *Pneumocystis carinii* MEKK, AAC21676 for *N. crassa* Nrc-1, and EAA73817 for *F. graminearum* FgSte11.

### ACKNOWLEDGMENTS

We thank Larry Dunkle, Stephen Goodwin, and Charles Woloshuk at Purdue University for critical reading of the manuscript and Chaoyang Xue and Kyeyong Seong for fruitful discussions. We also thank two anonymous reviewers for many constructive comments. This work was supported by a grant from the U.S. Department of Agriculture National Research Initiative and a grant from the National Science Foundation.

Received November 5, 2004; accepted January 27, 2005.

### REFERENCES

Adachi, K., and Hamer, J.E. (1998). Divergent cAMP signaling pathways regulate growth and pathogenesis in the rice blast fungus *Magnaporthe grisea*. *Plant Cell* **10**, 1361–1373.

- Andrews, D.L., Egan, J.D., Mayorga, M.E., and Gold, S.E. (2000). The *Ustilago maydis* *ubc4* and *ubc5* genes encode members of a MAP kinase cascade required for filamentous growth. *Mol. Plant-Microbe Interact.* **13**, 781–786.
- Banuet, F., and Herskowitz, I. (1994). Identification of *fuz7*, a *Ustilago maydis* MEK/MAPKK homolog required for a-locus-dependent and -independent steps in the fungal life cycle. *Genes Dev.* **8**, 1367–1378.
- Bardwell, L. (2004). A walk-through of the yeast mating pheromone response pathway. *Peptides* **25**, 1465–1476.
- Brachmann, A., Schirawski, J., Muller, P., and Kahmann, R. (2003). An unusual MAP kinase is required for efficient penetration of the plant surface by *Ustilago maydis*. *EMBO J.* **22**, 2199–2210.
- Brill, J.A., Elion, E.A., and Fink, G.R. (1994). A role for autophosphorylation revealed by activated alleles of *FUS3*, the yeast MAP kinase homolog. *Mol. Biol. Cell* **5**, 297–312.
- Bruno, K.S., Tenjo, F., Li, L., Hamer, J.E., and Xu, J.R. (2004). Cellular localization and role of kinase activity of *PMK1* in *Magnaporthe grisea*. *Eukaryot. Cell* **3**, 1525–1532.
- Chao, C.C.T., and Ellingboe, A.H. (1991). Selection for mating competence in *Magnaporthe grisea* pathogenic to rice. *Can. J. Bot.* **69**, 2130–2134.
- Chen, J.Y., Chen, J., Lane, S., and Liu, H.P. (2002). A conserved mitogen-activated protein kinase pathway is required for mating in *Candida albicans*. *Mol. Microbiol.* **46**, 1335–1344.
- Cherkasova, V.A., McCully, R., Wang, Y.M., Hinnebusch, A., and Elion, E.A. (2003). A novel functional link between MAP kinase cascades and the Ras/cAMP pathway that regulates survival. *Curr. Biol.* **13**, 1220–1226.
- Chumley, F.G., and Valent, B. (1990). Genetic analysis of melanin deficient, nonpathogenic mutants of *Magnaporthe grisea*. *Mol. Plant-Microbe Interact.* **3**, 135–143.
- Clarke, D.L., Woodlee, G.L., McClelland, C.M., Seymour, T.S., and Wickes, B.L. (2001). The *Cryptococcus neoformans* *STE11* alpha gene is similar to other fungal mitogen-activated protein kinase kinase (MAPKKK) genes but is mating type specific. *Mol. Microbiol.* **40**, 200–213.
- Cowley, S., Paterson, H., Kemp, P., and Marshall, C.J. (1994). Activation of MAP kinase kinase is necessary and sufficient for *PC12* differentiation and for transformation of NIH 3T3 cells. *Cell* **77**, 841–852.
- Csank, C., Schroppe, K., Leberer, E., Harcus, D., Mohamed, O., Meloche, S., Thomas, D.Y., and Whiteway, M. (1998). Roles of the *Candida albicans* mitogen-activated protein kinase homolog, Cek1p, in hyphal development and systemic candidiasis. *Infect. Immun.* **66**, 2713–2721.
- Dean, R.A. (1997). Signal pathways and appressorium morphogenesis. *Annu. Rev. Phytopathol.* **35**, 211–234.
- Di Pietro, A., Garcia-Maceira, F.I., Meglecz, E., and Roncero, M.I.G. (2001). A MAP kinase of the vascular wilt fungus *Fusarium oxysporum* is essential for root penetration and pathogenesis. *Mol. Microbiol.* **39**, 1140–1152.
- Dixon, K.P., Xu, J.R., Smirnov, N., and Talbot, N.J. (1999). Independent signaling pathways regulate cellular turgor during hyperosmotic stress and appressorium-mediated plant infection by *Magnaporthe grisea*. *Plant Cell* **11**, 2045–2058.
- Dohlman, H.G. (2002). G proteins and pheromone signaling. *Annu. Rev. Physiol.* **64**, 129–152.
- Grimshaw, S.J., Mott, H.R., Stott, K.M., Nielsen, P.R., Evetts, K.A., Hopkins, L.J., Nietlispach, D., and Owen, D. (2004). Structure of the sterile alpha motif (SAM) domain of the *Saccharomyces cerevisiae* mitogen-activated protein kinase pathway-modulating protein *STE50* and analysis of its interaction with the *STE11* SAM. *J. Biol. Chem.* **279**, 2192–2201.

- Gustin, M.C., Albertyn, J., Alexander, M., and Davenport, K. (1998). MAP kinase pathways in the yeast *Saccharomyces cerevisiae*. *Microbiol. Mol. Biol. Rev.* **62**, 1264–1300.
- Jenczmionka, N.J., Maier, F.J., Losch, A.P., and Schafer, W. (2003). Mating, conidiation and pathogenicity of *Fusarium graminearum*, the main causal agent of the head-blight disease of wheat, are regulated by the MAP kinase *GPMK1*. *Curr. Genet.* **43**, 87–95.
- Kaffarnik, F., Muller, P., Leibundgut, M., Kahmann, R., and Feldbrugge, M. (2003). PKA and MAPK phosphorylation of Prf1 allows promoter discrimination in *Ustilago maydis*. *EMBO J.* **22**, 5817–5826.
- Kahmann, R., and Kamper, J. (2004). *Ustilago maydis*: How its biology relates to pathogenic development. *New Phytol.* **164**, 31–42.
- Kim, Y.K., Kawano, T., Li, D.X., and Kolattukudy, P.E. (2000). A mitogen-activated protein kinase kinase required for induction of cytokinesis and appressorium formation by host signals in the conidia of *Colletotrichum gloeosporioides*. *Plant Cell* **12**, 1331–1343.
- Kohler, J.R., and Fink, G.R. (1996). *Candida albicans* strains heterozygous and homozygous for mutations in mitogen-activated protein kinase signaling components have defects in hyphal development. *Proc. Natl. Acad. Sci. USA* **93**, 13223–13228.
- Kothe, G.O., and Free, S.J. (1998). The isolation and characterization of *NRC-1* and *NRC-2*, two genes encoding protein kinases that control growth and development in *Neurospora crassa*. *Genetics* **149**, 117–130.
- Kranz, J.E., Satterberg, B., and Elion, E.A. (1994). The MAP kinase *Fus3* associates with and phosphorylates the upstream signaling component *Ste5*. *Genes Dev.* **8**, 313–327.
- Kusari, A.B., Molina, D.M., Sabbagh, W., Lau, C.S., and Bardwell, L. (2004). A conserved protein interaction network involving the yeast MAP kinases *Fus3* and *Kss1*. *J. Cell Biol.* **164**, 267–277.
- Lee, N., D'Souza, C.A., and Kronstad, J.W. (2003). Of smuts, blasts, mildews, and blights: cAMP signaling in phytopathogenic fungi. *Annu. Rev. Phytopathol.* **41**, 399–427.
- Lev, S., Sharon, A., Hadar, R., Ma, H., and Horwitz, B.A. (1999). A mitogen-activated protein kinase of the corn leaf pathogen *Cochliobolus heterostrophus* is involved in conidiation, appressorium formation, and pathogenicity: Diverse roles for mitogen-activated protein kinase homologs in foliar pathogens. *Proc. Natl. Acad. Sci. USA* **96**, 13542–13547.
- Li, L., Xue, C.Y., Bruno, K., Nishimura, M., and Xu, J.R. (2004). Two PAK kinase genes, *CHM1* and *MST20*, have distinct functions in *Magnaporthe grisea*. *Mol. Plant-Microbe Interact.* **17**, 547–556.
- Liebmann, C. (2001). Regulation of MAP kinase activity by peptide receptor signalling pathway: Paradigms of multiplicity. *Cell. Signal.* **13**, 777–785.
- Mayorga, M.E., and Gold, S.E. (1999). A MAP kinase encoded by the *ubc3* gene of *Ustilago maydis* is required for filamentous growth and full virulence. *Mol. Microbiol.* **34**, 485–497.
- Mayorga, M.E., and Gold, S.E. (2001). The *ubc2* gene of *Ustilago maydis* encodes a putative novel adaptor protein required for filamentous growth, pheromone response and virulence. *Mol. Microbiol.* **41**, 1365–1379.
- Mey, G., Oeser, B., Lebrun, M.H., and Tudzynski, P. (2002). The biotrophic, non-appressorium-forming grass pathogen *Claviceps purpurea* needs a *FUS3/PMK1* homologous mitogen-activated protein kinase for colonization of rye ovarian tissue. *Mol. Plant-Microbe Interact.* **15**, 303–312.
- Mitchell, T.K., and Dean, R.A. (1995). The cAMP-dependent protein kinase catalytic subunit is required for appressorium formation and pathogenesis by the rice blast pathogen *Magnaporthe grisea*. *Plant Cell* **7**, 1869–1878.
- Muller, P., Aichinger, C., Feldbrugge, M., and Kahmann, R. (1999). The MAP kinase *Kpp2* regulates mating and pathogenic development in *Ustilago maydis*. *Mol. Microbiol.* **34**, 1007–1017.
- Muller, P., Weinzierl, G., Brachmann, A., Feldbrugge, M., and Kahmann, R. (2003). Mating and pathogenic development of the smut fungus *Ustilago maydis* are regulated by one mitogen-activated protein kinase cascade. *Eukaryot. Cell* **2**, 1187–1199.
- Nishimura, M., Park, G., and Xu, J.R. (2003). The G-beta subunit *MGB1* is involved in regulating multiple steps of infection-related morphogenesis in *Magnaporthe grisea*. *Mol. Microbiol.* **50**, 231–243.
- Papadaki, P., Pizon, V., Onken, B., and Chang, E.C. (2002). Two Ras pathways in fission yeast are differentially regulated by two Ras guanine nucleotide exchange factors. *Mol. Cell. Biol.* **22**, 4598–4606.
- Park, G., Bruno, K.S., Staiger, C.J., Talbot, N.J., and Xu, J.R. (2004). Independent genetic mechanisms mediate turgor generation and penetration peg formation during plant infection in the rice blast fungus. *Mol. Microbiol.* **53**, 1695–1707.
- Ramezani-Rad, M. (2003). The role of adaptor protein *Ste50*-dependent regulation of the MAPKKK *Ste11* in multiple signalling pathways of yeast. *Curr. Genet.* **43**, 161–170.
- Ruiz-Roldan, M.C., Maier, F.J., and Schafer, W. (2001). *PTK1*, a mitogen-activated-protein kinase gene, is required for conidiation, appressorium formation, and pathogenicity of *Pyrenophora teres* on barley. *Mol. Plant-Microbe Interact.* **14**, 116–125.
- Takano, Y., Kikuchi, T., Kubo, Y., Hamer, J.E., Mise, K., and Furusawa, I. (2000). The *Colletotrichum lagenarium* MAP kinase gene *CMK1* regulates diverse aspects of fungal pathogenesis. *Mol. Plant-Microbe Interact.* **13**, 374–383.
- Talbot, N.J. (2003). On the trail of a cereal killer: Exploring the biology of *Magnaporthe grisea*. *Annu. Rev. Microbiol.* **57**, 177–202.
- Thines, E., Weber, R.W.S., and Talbot, N.J. (2000). MAP kinase and protein kinase A-dependent mobilization of triacylglycerol and glycogen during appressorium turgor generation by *Magnaporthe grisea*. *Plant Cell* **12**, 1703–1718.
- Valent, B., and Chumley, F.G. (1991). Molecular genetic analysis of the rice blast fungus, *Magnaporthe grisea*. *Annu. Rev. Phytopathol.* **29**, 443–467.
- Xu, H.P., White, M., Marcus, S., and Wigler, M. (1994). Concerted action of Ras and G-proteins in the sexual-response pathway of *Schizosaccharomyces pombe*. *Mol. Cell. Biol.* **14**, 50–58.
- Xu, J.R., and Hamer, J.E. (1996). MAP kinase and cAMP signaling regulate infection structure formation and pathogenic growth in the rice blast fungus *Magnaporthe grisea*. *Genes Dev.* **10**, 2696–2706.
- Xu, J.R., Staiger, C.J., and Hamer, J.E. (1998). Inactivation of the mitogen-activated protein kinase *Mps1* from the rice blast fungus prevents penetration of host cells but allows activation of plant defense responses. *Proc. Natl. Acad. Sci. USA* **95**, 12713–12718.
- Xu, J.R., Urban, M., Sweigard, J.A., and Hamer, J.E. (1997). The *CPKA* gene of *Magnaporthe grisea* is essential for appressorial penetration. *Mol. Plant-Microbe Interact.* **10**, 187–194.
- Zhao, X., Xue, C., Kim, Y., and Xu, J.R. (2004). A ligation-PCR approach for generating gene replacement constructs in *Magnaporthe grisea*. *Fungal Genet. Newsl.* **51**, 17–18.
- Zheng, L., Campbell, M., Murphy, J., Lam, S., and Xu, J.R. (2000). The *BMP1* gene is essential for pathogenicity in the gray mold fungus *Botrytis cinerea*. *Mol. Plant-Microbe Interact.* **13**, 724–732.